

A&A 631, A67 (2019)
<https://doi.org/10.1051/0004-6361/201936059>
© ESO 2019

**Astronomy
&
Astrophysics**

Inversion of HIPPARCOS and *Gaia* photometric data for asteroids

Asteroid rotational properties from sparse photometric data

A. Cellino¹, D. Hestroffer², X.-P. Lu³, K. Muinonen^{4,5}, and P. Tanga⁶

¹ INAF, Osservatorio Astrofisico di Torino, Via Osservatorio 20, 10025 Pino Torinese, Italy
e-mail: alberto.cellino@inaf.it

² IMCCE, Observatoire de Paris, Université PSL, CNRS, Sorbonne University, Université Lille, 75014 Paris, France
e-mail: Daniel.Hestroffer@imcce.fr

³ Macau University of Science and Technology, Macau, PR China
e-mail: xplu@must.edu.mo

⁴ Department of Physics, University of Helsinki, Gustaf Hällströmin katu 2a, PO Box 64, 00014 U. Helsinki, Finland

⁵ Finnish Geospatial Research Institute FGI, Geodeetinrinne 2, 02430 Masala, Finland

⁶ Université Côte d'Azur, Observatoire de la Côte d'Azur, CNRS, Laboratoire Lagrange, Boulevard de l'Observatoire, CS34229, 06304 Nice Cedex 4, France

Received 10 June 2019 / Accepted 27 August 2019

ABSTRACT

Context. Sparse photometric data can be used to determine the spin properties and infer information about the shapes of asteroids. The algorithm adopted for the inversion of *Gaia* photometric data assumes, for the sake of simplicity and to minimize CPU execution time, that the objects have triaxial ellipsoid shapes. In the past, this algorithm was tested against large sets of simulated data and small numbers of sparse photometric measurements obtained by HIPPARCOS.

Aims. After the second *Gaia* data release, it is now possible to test the inversion algorithm against small samples of actual *Gaia* data for the first time. At the same time, we can attempt a new inversion of older HIPPARCOS measurements, using an updated version of the photometric inversion algorithm.

Methods. The new version of our inversion algorithm includes the treatment of a Lommel-Seeliger scattering relation especially developed for the case of triaxial ellipsoid shapes. In addition, we also performed inversion attempts using a more refined shape model, based on the so-called cellinoid shapes.

Results. With respect to the old inversion of HIPPARCOS data carried out in the past, we obtain only marginal improvements. In the case of *Gaia* data, however, we obtain very encouraging results. A successful determination of the rotation period is possible in most cases, in spite of the limited time span covered by data published in the second *Gaia* data release (GDR2), which makes the determination of the spin axis direction still uncertain. Even a small number of measurements, less than 30 in many cases, are sufficient to obtain a satisfactory inversion solution. Using the more realistic cellinoid shape model, we find further improvement in the determination of the spin period.

Conclusions. This is a relevant validation of GDR2 photometry of asteroids, and proof of the satisfactory performances of the adopted inversion algorithm.

Key words. methods: data analysis – techniques: photometric – minor planets, asteroids: general

1. Introduction

The recent second data release of *Gaia* measurements (hereinafter GDR2) for the first time included astrometric and photometric data for a sample of about 14 000 solar system objects; in the vast majority of cases these objects are asteroids ([Gaia Collaboration 2018](#)). Such sparse photometric measurements can in principle be inverted to derive information from them about the rotational properties (i.e. spin period and orientation of the spin axis), the overall shape, and some light-scattering properties (i.e. relation between magnitude and phase angle¹) of the observed objects, taking advantage of the supposedly high accuracy of *Gaia* measurements. This is one of the main goals of the exploitation of *Gaia* photometric observations of asteroids, but in GDR2 the number of single measurements obtained for each

single target is in the vast majority of cases still small, and this challenges a priori any attempt of photometric inversion. Moreover, the interval of time covered by GDR2 data is less than two years, from August 5, 2014 to May 23, 2016. This means that the variety of observing circumstances, in terms of coverage of the ecliptic longitude of the objects, which in turn determines the interval of aspect angles² covered by the observations, is still very limited.

In preparation for the release of *Gaia* photometric data for solar system objects, some of us developed an algorithm of photometric inversion that has been implemented by the Data Processing and Analysis Consortium (DPAC), which is in charge of performing the operations of *Gaia* data reduction and preliminary processing. The computation is based on an algorithm using a simple shape model, namely a regular triaxial ellipsoid shape,

¹ The phase angle is the angle between the directions to the Sun and to the observer, as seen from the observed object.

² The aspect angle is the angle between the direction of the spin axis of the object and the target-observer direction.

to minimize the execution time. This approach has been extensively tested by means of numerical simulations (Carbognani et al. 2012; Cellino et al. 2015), the most recent results having been published by Santana-Ros et al. (2015), who found that the most difficult situations for photometric inversion are those of asteroids having very low values of the ecliptic latitude of the pole, mostly as an unavoidable consequence of the choice of a very simple and symmetric shape model. The results of a test – based on simulations and actual sparse photometric data obtained in the 1980s by the High Precision PARallax COLlecting Satellite (HIPPARCOS) – had been previously presented by Cellino et al. (2009). The results of this analysis were fairly encouraging. A correct determination of the spin period was obtained in about one-half of the cases by inversion of HIPPARCOS data. This even though these measurements were affected by quite large error bars, most often of the order of 0.05 mag, and were also fairly limited in terms of the number of available measurements per object (about 50 measurements per object; see Hestroffer et al. 1998; Lu et al. 2016).

The availability of the first *Gaia* photometric data published in GDR2 for the first time allows us to test the inversion algorithm against the data this algorithm is designed to process. At the same time, the inversion algorithm has been further improved with respect to the version adopted by Cellino et al. (2009) because in its current version it includes a better treatment of light scattering effects. Taking this improvement into account, we can also refresh our analysis of HIPPARCOS photometric data to check whether the results of the previous photometric inversion can be improved by a better treatment of light scattering.

This paper is organized as follows: in Sect. 2, we summarize the general characteristics of the problem of inversion of sparse photometric data. In Sect. 3 we briefly discuss some properties of the data we use in our analysis. In Sect. 4 we describe the inversion algorithm used in our analysis, in particular stressing some improvements we recently made. In Sect. 5 we describe an alternative and more realistic shape model that we test in a number of cases to check how the results of photometric inversion can improve. The results of our analysis are shown and discussed in Sect. 6. The final conclusions are summarized in Sect. 7.

2. Inversion of sparse photometric data for asteroids

The most usual situation encountered in asteroid photometry is that of many observations covering one or a few consecutive nights in such a way as to obtain a so-called light curve, which is a record of the photometric variation, caused by a non-spherical shape, of an object spinning around its rotation axis. For asteroids above 150 m in size, the range of possible rotation periods is between about 2.2 h, corresponding to the so-called spin barrier (Pravec & Harris 2000), up to several tens of hours. In the vast majority of cases, however, the rotation periods are found to be between 4 and 12 h (Pravec et al. 2002). The amplitude of one single light curve can also provide some qualitative estimate of the shape of the object; increasingly larger light curve amplitudes suggest increasingly elongated shapes. Normally, further information about the shape and spin state of an object (including the orientation of its rotation axis) can be derived by obtaining light curves at different epochs, corresponding to different configurations of the target – observer – Sun mutual positions. Many sophisticated algorithms have been developed by different authors to derive accurate shape and spin

state solutions for objects for which multiple light curves are available (see, for a review, Āurech et al. 2015).

The same information however is also present, although somehow diluted, in a set of sparse photometric measurements (“snapshots”) taken at different epochs. Of course, all apparent magnitudes must be preliminarily converted to values corresponding to unit distance from the Sun and from the observer. The (reduced) magnitude of any given object varies over a shorter timescale corresponding to its spin period and over longer timescales because the orbital motion and direction of the spin axis produce a progressive change of brightness; this is because the object presents different illuminated cross sections of its shape to the observer at different epochs. It is also normally assumed that the object is in a state of free rotation around the axis of maximum moment of inertia and is not affected by any kind of precessional motion. It is then possible to analyse a set of sparse photometric measurements of the same object and to derive from these the same information that can be obtained by full light curves. Of course, it is important that all the photometric data are accurate because even small errors in some data points can easily have important consequences on the final inversion solutions.

The inversion can be done by imposing a priori a given shape model for the object, which can be suitable if the number of available measurements is small. In most favourable cases, a complex shape can be determined simultaneously with the spin properties. In general terms, it is advisable that all the data are obtained using a unique instrument and detector to avoid the problem of merging together data affected by different systematic and random errors because of the use of different hardware working in different sky conditions. The ideal situation is therefore to use data obtained by one single observing platform located in space. In this respect, the cases of the photometric data obtained years ago by HIPPARCOS, as well as the data currently produced by the *Gaia* mission, are absolutely ideal for the purposes of photometry inversion.

There are obvious constraints concerning the quantity and quality of the sparse photometric data available for analysis. Needless to say, larger numbers of measurements and better photometric accuracy produce better inversion results. In more quantitative terms, based on a large body of numerical simulations, Cellino et al. (2009) discussed which cases can be typically inverted, and which cannot, based on conditions given in terms of number of measurements versus average photometric errors. According to these authors, 20 well-distributed observations with photometric uncertainties smaller than 0.01 mag should be sufficient to carry out successful inversions of bodies that have triaxial ellipsoid shapes. In the latter work, well distributed means observations covering a sufficiently wide variety of aspect angles. In turn, this normally corresponds to ground-based observations covering a time span of the order of four or five years. Of course, the assumption of objects with ideal triaxial ellipsoid shapes is a severe approximation because it is clear that real objects do not have these kinds of shapes; however it seems that a triaxial ellipsoid shape approximation is not so bad in many cases, according to Torppa et al. (2008, 2006). It is clear, therefore, that when dealing with real objects, the conditions of successful photometric inversion can be expected to be much more severe in terms of required number and accuracy of the available observations. Neither constraints are met when dealing with the HIPPARCOS asteroid photometric data, whereas the constraint concerning photometric accuracy is expected to be met in the case of GDR2 data. In this case, however, the

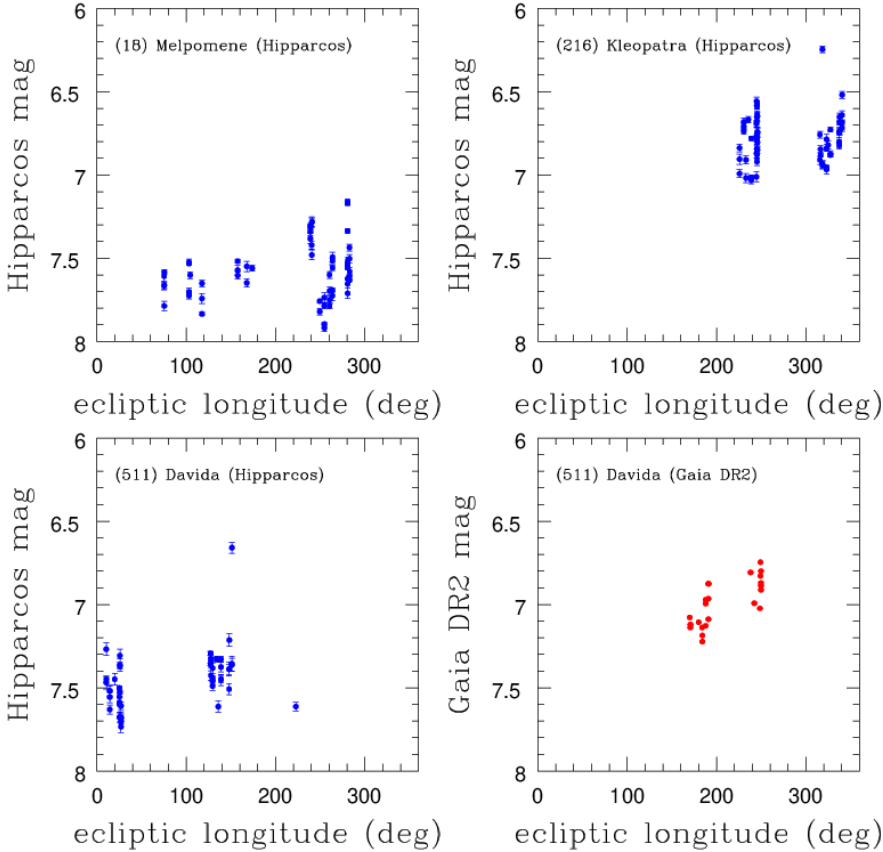


Fig. 1. Magnitude vs. ecliptic longitude for three sets of HIPPARCOS asteroid data: asteroids (18), (216), and (511), and one set of GDR2 data for asteroid (511).

number of observations and their distribution in terms of observing circumstances are in general still far from satisfactory. Some examples of these features are represented in Fig. 1, showing a few typical cases. The HIPPARCOS and *Gaia* data for the asteroid (511) Davida are shown side by side in the bottom line of the figure to make a comparison easier. It is easy to see that in the case of HIPPARCOS data, the coverage in terms of ecliptic longitude (corresponding to 3.5 yr of mission) is better than in the case of *Gaia* data (covering only 1.5 yr). But the inversion of HIPPARCOS data was not successful for (511) Davida, whereas the GDR2 data led us to find the correct spin period. In the case of HIPPARCOS data a purely visual inspection is sufficient to identify some data that look suspect because they are much different (brighter in the cases of (216) and (511) shown in Fig. 1) than the rest of the available measurements taken at a similar ecliptic longitude. Even by removing these data, however, we could not obtain a correct inversion solution. We note also that owing to the adopted scale, Fig. 1 hardly shows another important difference between the HIPPARCOS and GDR2 data sets, namely the fact that HIPPARCOS data are affected by much larger error bars. In the case of GDR2 data for (511) Davida shown in the figure, the error bars are smaller than the red symbols adopted to represent the data.

3. Available data

The HIPPARCOS data used in the present analysis are exactly the same as those used by Cellino et al. (2009), and they are no longer discussed in what follows. We note that the photometric accuracy of these data, obtained in the so-called H_p band, was not accurate enough for the purposes of photometry inversion because these data usually have uncertainties, which are in many

cases likely underestimated, of the order of 0.03 mag or even worse.

In the case of GDR2 photometric data, a synthetic presentation is given by Gaia Collaboration (2018), while many more details are given in the online document by van Leeuwen et al. (2018). In particular, the nominal photometric accuracy of these data is much better than in the case of HIPPARCOS, as the accuracy is often better than 0.01 mag, at least for the sample of objects considered in this analysis. A very important property of *Gaia* photometric data is that they are obtained in the *Gaia* G photometric system, which is different from the HIPPARCOS H_p photometric system. In principle, it would be interesting to merge together HIPPARCOS and *Gaia* data for the same objects. To do this, a conversion of all data to a common photometric system would be needed. The most convenient choice would be to convert GDR2 data into the HIPPARCOS H_p system. As explained in van Leeuwen et al. (2018), this can be done according to a simple relation, which is a function of the G magnitude and of the colours of the objects, recorded by the B and R *Gaia* detectors. Unfortunately, this conversion cannot be done at this stage, simply because no colour data for solar system objects were published in GDR2. An opposite inversion from the HIPPARCOS to the *Gaia* photometric system could be done in principle, and the corresponding form of this transformation, which depends upon the $(B-V)$ or $(V-I)$ HIPPARCOS colours, has also been published in van Leeuwen et al. (2018). Unfortunately, the problem in this case is that the measurements of the colours for the asteroids observed by HIPPARCOS in its own photometric system are affected by exceedingly large uncertainties to be used in practice. As a consequence, we are forced to keep the HIPPARCOS and *Gaia* observations distinct and to process these independently. In this respect, the situation will be much better in

the next *Gaia* data release, when not only will the *Gaia* colours of small solar system objects be published, making a conversion to the HIPPARCOS photometric system possible, but the number of photometric measurements per object will also be much higher.

For the moment, we limited our analysis to cases in which the number of available HIPPARCOS measurements are sufficient to justify an inversion attempt. Based on a large body of simulations and on the results published by Cellino et al. (2009), this number has been set to 25.

We also note that our analysis is in many respects similar to an independent work carried out by Āurech & Hanus (2018) using only GDR2 data. A major difference is that the above authors attempted a determination of the spin period for a much larger sample of asteroids present in the GDR2 catalogue, choosing all those with a minimum number of observations equal to 10. Their results confirm our expectations that, when the number of observations is smaller than 20, correct values of the rotation period cannot be obtained for measurements that have the photometric accuracy of GDR2 data, even making use of more sophisticated shape models.

4. Inversion algorithm for the triaxial shape model

We have developed an approach based on a genetic algorithm to carry out an inversion of sparse photometric data; this algorithm has been described in different papers, including Cellino et al. (2006, 2009) and Santana-Ros et al. (2015). By assuming that the asteroid has a shape corresponding to a regular triaxial ellipsoid, the basic idea is that the algorithm begins to mimic a genetic evolution of the solutions, starting from a randomly chosen set of the unknown parameters; these parameters are the spin period, ecliptic longitude and latitude of the pole, two axial ratios, a parameter describing a linear variation of magnitude as a function of phase angle, and a value of the rotation angle of the object at a reference epoch. This is done by generating new solutions from single mutations of a randomly chosen parent solution or from a random assignment of the parameters taken from those of a couple of parent solutions. Every generated solution can be accepted or discarded based on the criterion of producing smaller residuals with respect to those of the worst solution belonging to the previous generation (that is discarded in this case). The set of possible solutions evolve in this way after some generation cycles, up to the point that a final, stable best solution (namely a set of parameters minimizing the residuals) is found. In other words, a minimum value of the root mean squared ($O-C$) is reached and cannot be improved by further iterations. Owing to its intrinsic mechanism, we cannot guarantee that the right solution can be found after just one single “genetic attempt”, which for us means a number of the order of several cycles of generation of 10 000 solutions starting from a fully random set. Multiple attempts must be performed to check that the same best inversion solution is found in more than just one attempt. In this respect, we note that the chosen value for the maximum number of different genetic attempts is determined by a compromise between the need to maximize the number of attempts and the need to minimize the necessary execution time. In this analysis, we set the maximum number of genetic attempts to 20. The corresponding execution time depends upon the amount of available photometric data used for the inversion; this time span is generally a couple of minutes using a commercial desktop computer that is a few years old. In analysing how this choice can affect the quality of the inversion results, we found that there can be some difficult situations in which the

right period solution is found only once or more than one best solution share equivalent residuals. These cases represent some exceptions to the normal situation. As far as we can understand, these are cases in which the chance of obtaining the correct solution is severely reduced because of the shape of the object, the low amount of observational data, and most probably the still insufficiently wide distribution of the data in the space of observing circumstances. This is particularly true taking into account that, using a simple triaxial ellipsoid shape model, some 180° ambiguity in the determination of the ecliptic longitude of the pole may arise if the pole latitude is near to zero, and/or if the orbit of the asteroid has a very small inclination with respect to the ecliptic. The same cases, on the other hand, can often (but not always) be inverted using a more sophisticated shape model, as we see below.

We expect that the objects that we cannot invert now using GDR2 data will be successfully inverted using the triaxial shape model as soon as larger numbers of observations made in different observing conditions become available in the next *Gaia* data releases. For the moment, we consider as solid inversion solutions, using the triaxial shape model, those for which the correct solution is found more than once in the set of 20 genetic attempts performed in this analysis. Correct solutions obtained in just one attempt must be considered of lower quality.

We also note that at this stage, in which GDR2 data are still poor in terms of covered aspect angles, it would be unreasonable to expect to be already able to obtain full solutions for period, pole, and overall shape. For this reason, when analysing the results of our inversions of GDR2 data, we consider those inversions leading to a correct determination of the spin period as successful; we require therefore that our spin period solutions are within a few seconds from the values determined through years of ground-based photometry. We consider the associated pole solution as an ancillary result, for which we can expect, at least in some cases, significant uncertainties and errors at this stage.

We also note that our genetic algorithm of photometry inversion of triaxial ellipsoid shapes looks for a simultaneous solution of the spin period and all the other unknown parameters. This is different with respect to the majority of different inversion techniques, in which the determination of the spin period is done separately and before the determination of pole and shape (see e.g. Āurech & Hanus 2018, and references therein).

5. Alternative shape model

We are aware that the adoption of a triaxial ellipsoid shape is inherently simplistic. It has been dictated by the practical need of limiting, to a minimum, the execution time needed to carry out the inversion of *Gaia* photometric data, for a number of objects of the order of 10^5 at the end of the mission, to determine for these objects the spin properties (rotation period, pole axis orientation, and sense of spin) and some indication of the general shape. The advantage of the triaxial ellipsoid shape is that the computation of the visible and illuminated area of an object seen in any observing condition can be computed by means of analytical relations. The price to pay is a simplistic shape solution, but on the other hand a very accurate determination of the shape is beyond the scope of *Gaia*; at the same time years of numerical simulations have shown that the period and pole solutions obtained using a triaxial ellipsoid shape are generally not affected by unacceptable errors. In this paper, we analyse the kind of improvement that we can expect in the inversion solutions by considering more realistic shape models.

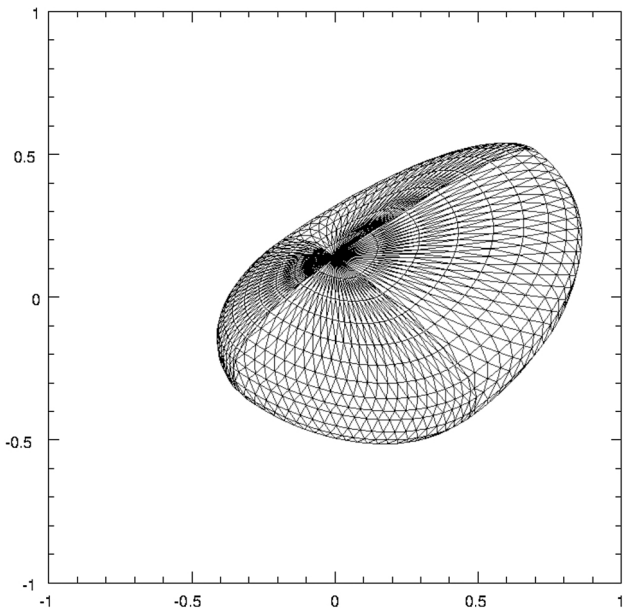


Fig. 2. Cellinoid with semi-axes $a_1 = 1.0$, $a_2 = 0.5$, $b_1 = 0.7$, $b_2 = 0.3$, $c_1 = 0.4$, $c_2 = 0.2$, seen as rotated by 45° around its spin axis, and at an aspect angle of 45° . The triangular facets have base widths of 10° in longitude, and heights of 5° in latitude.

There are many possible choices if we want to relax the constraints of a simple symmetric shape. The most general choice can be that of not assuming a priori a given shape model, but to look for a general convex shape that best fits the available data. In recent years several authors have taken this approach, including Hanuš et al. (2016) and Ďurech et al. (2016, 2018). A simpler possibility, that we adopt in this paper, is the choice of another kind of fixed shape model that is much more flexible than a regular triaxial ellipsoid. We chose therefore a so-called cellinoid shape model, thus named because such a shape model was adopted for the first time by Cellino et al. (1989). A cellinoid is the most immediate generalization of a triaxial ellipsoid and consists of the merging of eight different octants of regular triaxial ellipsoids with different lengths of their semi-axes, but chosen in such a way that adjacent octants share the same semi-axes. It is therefore characterized by six different values for the semi-axes: a_1 , a_2 , b_1 , b_2 , c_1 , and c_2 . An example is given in Fig. 2. In this way, it is possible to consider shapes that can be far from symmetry, thereby avoiding some of the most important limitations of a regular triaxial shape. Of course, since a cellinoid is not symmetric, the direction of its rotation axis is not as trivial as in the case of regular triaxial ellipsoids, but it must be computed through a diagonalization of the inertia tensor.

The use of a cellinoid shape model was extensively explained by Lu et al. (2016), who gave a thorough description of their adopted procedures. A major difference with respect to the inversion algorithm adopted to treat triaxial ellipsoid shapes, as explained in Sect. 4, is that in the case of the cellinoid shape model a solution is found first for the spin period; only subsequently the search for the pole and shape solution is executed, by considering a grid of points on the celestial sphere to find the smallest possible residuals with the available observations using a Levenberg-Marquardt algorithm. In other words, in contrast to the genetic algorithm used in treating triaxial ellipsoid shapes, our treatment of cellinoid shapes is a locally optimized method.

Lu et al. (2016) presented the results of their photometry inversions of 11 asteroids belonging to the same set of

HIPPARCOS photometric data analysed by Cellino et al. (2009). The former results were compared with both the results of Cellino et al. (2009) for the same objects and with the results of inversions based on an extensive analysis, by Ďurech et al. (2010), of light curves included in the Database of Asteroid Models from Inversion Techniques (DAMIT), database, a list of three-dimensional models of asteroids computed using inversion techniques, maintained and operated by The Astronomical Institute of the Charles University in Prague, Czech Republic. This comparison was found to be very encouraging because the obtained inversions agree well with those of extensive ground-based data, and are also successful in the cases of some asteroids for which Cellino et al. (2009) were not able to find a solution. This was interpreted as an expected result because of the use of a more flexible shape model, although at the cost of a significant amount of processing time. In some cases, moreover, it was found that more than two possible pole solutions can be practically equivalent in terms of residuals.

6. Results and uncertainties

In this section we give the results of our photometric inversion exercises of HIPPARCOS and GDR2 data. In evaluating the success or failure of an inversion of GDR2 data, we consider primarily the agreement with the rotation period determined by many years of ground-based photometry, and we only marginally consider the obtained pole solutions. This is because spin periods for the objects of our data set have been accurately determined from many light curves obtained over the years by various ground-based observers, and therefore are highly reliable and accurate.

At this stage however we do not consider our obtained pole solutions as really indicative of the quality of photometric inversion, for two main reasons. First, the determination of the orientation of the spin axis, namely the pole coordinates, is not straightforward. Particularly in the case of GDR2 data, but also frequently when dealing with HIPPARCOS data, the available, sparse photometric data are not sufficient to cover a variety of observing circumstances (aspect angles) sufficient to derive reliable pole estimates. While in the case of HIPPARCOS data there is nothing we can do, in the case of *Gaia* data the situation will certainly improve with time because larger numbers of photometric measurements taken at different epochs will accumulate for each object until the end of the mission. Second, in about 20% of the considered objects, no pole solution is available in the literature. In the remaining cases, moreover, the asteroid pole has been generally determined independently by several authors using different techniques, and different possible pole solutions have correspondingly been found; these differing approaches are often hardly compatible with each other. It would be impractical to list, in the tables, a summary of our results of all the possible alternative pole solutions found using ground-based data for each object.

For these reasons, in Tables A.1–A.3, which summarize the results of our inversion procedures, we consider as successful the inversions leading to a correct determination of the spin period. We take as “true” value of the rotation period for each object the value given in the Asteroid Lightcurve Data Base (ALDB) available at the Planetary Data System Small Bodies Node³ (Pravec & Harris 2018). The accuracy in the knowledge of the period varies for different objects. It can be extremely high, as in the case of asteroids visited by space probes, such as (4) Vesta, whose

³ Available at <https://sbn.psi.edu/pds/resource/lc.html>

period expressed in hours is known with a precision of eight digits, but most often it is given with three digits, corresponding to an uncertainty of 3.6 s. In our inversion computations we find that differences of 0.0001 h in the computed period generally correspond to non-negligible differences in the solution residuals. For this reason, in Tables A.1–A.3 we express the period solutions in hours with a precision of four digits; we consider as correct the period solutions corresponding to differences of only few seconds with respect to the value listed in ALDB, or slightly more in the cases of objects that have periods longer than ten hours. This empirical approach also seems to be justified by the fact that similar period uncertainties can be expected to affect the values listed in the ALDB database, which summarizes the determinations obtained by different observers.

For what concerns the obtained pole coordinates, we only indicate whether they are generically in agreement with at least some published ground-based estimates. We note that the obtained pole solutions tend to be in very reasonable agreement in several cases, say within about 20° , with pole solutions published in the literature. Using a regular triaxial shape model, the most important discrepancy is given most often by a 180° ambiguity in the resulting ecliptic longitude of the pole, but this is not unexpected because of intrinsic limitations of the adopted shape model, as pointed out by [Santana-Ros et al. \(2015\)](#). In the case of the inversions using the cellinoid shape model, we find a larger number of successful determinations of the spin period, but at the same time the obtained pole solutions are generally more distant from values published in the literature, and in several cases the sense of rotation appears to be inverted, for reasons that are still not completely understood.

The determination of the uncertainties of the solution parameters found by photometric data inversion is generally not straightforward, especially when using a genetic algorithm. In fact, when computing an inversion solution corresponding to an assumed shape model, what is obtained is a set of values for the unknown parameters, which produces the best possible fit of the given data, for an object with the adopted shape model. A formal computation of the nominal errors of the solution parameters, therefore, can lead to misleading results, when it is clear that the largest part of the real error budget is due to the use of an inadequate shape model. Years of numerical simulations have convinced us that the real errors in the determination of the pole coordinates can hardly be assumed to be less than about 10° , when assuming a triaxial ellipsoid shape model, even when an analysis of the pole solutions over very large numbers of genetic attempts would suggest smaller uncertainties. As for the shape, since we know a priori that a triaxial ellipsoid shape model is only a first-order approximation, the nominal uncertainty on the resulting axial ratios is not really very important, and can only be used to acquire qualitative information about the general oblateness of the body. In the case of GDR2 data, in which we make inversions of very small numbers of sparse measurements, we think that it is still premature to look for accurate determinations of the uncertainties in the solution parameters; we postpone this task to the end of the *Gaia* mission when all the transits of the objects during the whole mission lifetime have been measured and recorded. As for the rotation period, which is the fundamental solution parameter we are considering in the present analysis, we find that small changes, of the order of 10^{-3} h, produce variations in the resulting solution residuals which are generally very small, but already sufficient to make the difference between a correct and a wrong period solution most often. Based on our experience, the most important difference between a correct and wrong solution, is that in the former case we obtain the

same period solution more than once through different genetic attempts, and this solution tends to produce average residuals lower by more than 0.001 mag with respect to the remaining solutions. When the above conditions are not met, the inversion solution giving the smallest residuals is often wrong. In some cases the correct solution may be present among a number of different solutions sharing nearly identical residuals, but there is no possibility to identify it among these solutions. In Tables A.1–A.3, therefore, we do not list estimates of the error bars in our obtained inversion solutions. We assume that in all cases the uncertainties in the determination of the spin period are of the order of a few seconds of time, as mentioned above. In the case of the inversion of HIPPARCOS data we list the obtained pole solutions in addition to the rotation periods, but we know that the solution uncertainties for the poles are large because of the overall bad quality of HIPPARCOS data.

We note that the determination of the inversion solution errors is not a trivial task even using more sophisticated photometry inversion algorithms aimed at computing a best-fit convex shape from the available data (instead of assuming it a priori). See, for instance, [Ďurech & Hanus \(2018\)](#) and references therein.

6.1. HIPPARCOS data

We limited our analysis of HIPPARCOS data to the cases of objects for which the number of HIPPARCOS measurements is >25 . The only one notable exception is given by (216) Kleopatra because at the epoch of the [Cellino et al. \(2009\)](#) paper it was already discovered that a correct inversion can be obtained for this object in spite of a tiny number of observations (only 19). This is probably a consequence of the fact that Kleopatra has a very elongated shape, producing a strong modulation of the photometric signal, which makes it easier to determine the spin period.

6.1.1. Triaxial ellipsoid shape model

The results of this new analysis of HIPPARCOS data are given in Table A.1 and can be summarized very easily. Apart from a very few cases, no significant differences are found with respect to the results obtained by [Cellino et al. \(2009\)](#). An improvement is given by the fact that this time we obtain a correct determination of the spin period of (18) Melpomene, with two possible pole solutions, one of which is in extremely good agreement with that published by [Hanus et al. \(2016\)](#).

Our inversion of photometric data of the big asteroid (4) Vesta finds a rotation period that is nearly equal to twice the value found from ground-based light curves. This is not unexpected, and was already found by [Cellino et al. \(2009\)](#). The explanation is that it is known that in the case of Vesta a large-scale albedo variegation, rather than the shape, is mostly responsible for the observed light curves ([Cellino et al. 2016](#), and references therein). It is interesting that in this new analysis of HIPPARCOS data we also find in the case of (6) Hebe a rotation period practically equal to twice the value found from ground-based light curves. We cannot rule out the possibility that for this object some heterogeneity in surface albedo, as also suggested by [Migliorini et al. \(1997\)](#), could also be responsible for the photometric variation.

Finally, in spite of a supposedly better treatment of light scattering effects, we no longer find for the two asteroids (3) Juno and (354) Eleonora period solutions close to published values. The nominal solutions found by [Cellino et al. \(2009\)](#) however

were very uncertain and, at least in the case of Juno, included a very elongated and not very realistic shape for this big asteroid.

We note that, with respect to the inversion code used by Cellino et al. (2009), the main difference in the current version is a better treatment of the light scattering effects, since we now use a Lommel-Seeliger scattering model especially computed for the case of triaxial ellipsoid shapes (Muinonen et al. 2015; Cellino et al. 2015). The results of the current analysis suggest that the treatment of light scattering effects are not of primary importance in the case of HIPPARCOS data because the error budget is probably dominated by insufficient accuracy of the data, possibly coupled with a simplistic shape model, rather than by the role played by light scattering.

We note however that although the inversion solutions for the spin period have remained essentially unchanged, some general, although limited, improvements seem to be present for what concerns a slightly better average agreement with the most recently published pole solutions.

6.1.2. Cellinoid shape model

As mentioned above, the results of an inversion of a sub-sample of 11 asteroids included in the HIPPARCOS data set were already presented by Lu et al. (2016). In this paper we consider a significantly larger number of objects. The results are listed in Table A.2. These findings show that the correct spin period was obtained for 15 out of 38 objects, including as a good period solution also that obtained for Vesta, which is equal to twice the correct value, but acceptable for the reasons explained in Sect. 6.1.1. The number of good inversions is therefore very similar to the case of inversions using the triaxial ellipsoid shape model. With respect to the pole solutions, the situation is slightly worse. In general, there is little agreement with either the values found in the literature or the solutions shown in Table A.1 for inversions using the triaxial shape model. We have so far not found an explanation for this behaviour. We note that using the current algorithm the computation of the spin period is separated from the search of the pole and shape solution. At this stage we can conjecture that the HIPPARCOS data are affected by so many and large errors that inversion attempts using a sophisticated shape model can be more affected than in the case of using a simpler triaxial ellipsoid shape. It is even possible that some algorithms used in the inversion code using cellinoid shapes could be improved, possibly including a more accurate determination of the direction of the axis of maximum inertia. It is also possible that increasing the number of nodes of the grid on the celestial sphere used to find the best-fitting pole solution could avoid missing narrow minima in the residuals and correspondingly improve the pole solution.

6.2. *Gaia* Data Release 2 data

As explained above, we limited our analysis of new GDR2 data to a small number of asteroids, namely all those numbered up to 500 that have more than 25 GDR2 recorded data. This corresponds to a sample of 39 objects. The nominal photometric errors for these data were in all cases extremely low; in a large number of cases these errors were better than 0.01 mag. Our sample is much smaller than that analyzed by Ďurech & Hanus (2018), who considered 5413 asteroids having a number of GDR2 photometric measurements ≥ 10 . According to the above authors, however, in the vast majority of the cases no good period solution could be obtained, and an inversion solution was found for only 173 objects. This number is certainly much larger than our

sample of 39 asteroids, but the essential results of our analysis are in very good agreement with those by Ďurech & Hanus (2018). In terms of direct comparison of inversion solutions, however the intersection between the two samples is extremely small (only two objects).

6.2.1. Triaxial ellipsoid shape model

The results of our inversion attempts using the triaxial ellipsoid shape model are listed in Table A.3, in which we also list the results of our inversion of GDR2 data for two asteroids included in the HIPPARCOS asteroid database: namely (216) Kleopatra, for which we have only 17 GDR2 measurements, and (511) Davida, for which 23 GDR2 observations are available. It is easy to see that the obtained results are very encouraging. The correct period solution is found in 23 out of 39 cases despite the small number of observations per object available in most cases and the correspondingly poor variety of observational circumstances due to the limited time span covered by GDR2 observations (22 months). We also note that in several cases, which we consider as unsuccessful, we found a number of different solutions, which we consider equivalent in terms of residuals; these also include the correct spin period in some cases. We are confident that for these objects, future *Gaia* data releases with many more observations will be decisive to derive unequivocally the correct inversion solution.

The number of available measurements does not seem to be the most important parameter determining the success of photometric inversion because in some cases we could invert objects with less than 30 observations, whereas in a couple of cases we could not invert objects with more than 40 measurements. The derived pole coordinates, in cases in which some well-established result from ground-based data was available, are in general in reasonable agreement (around 20°) with published pole solutions. In a number of cases, we find a 180° ambiguity in the determination of the longitude of the pole, but this is a well-known problem using a triaxial ellipsoid shape model. In a couple of cases, for asteroids (295) and (411), we obtain period solutions equal to twice the periods derived from ground-based data. It is not clear whether this could be due to insufficient data or to possible albedo heterogeneity of the surfaces of these two objects. We also note that in the cases of several unsuccessful inversions, no pole solution is known from ground-based observations. This might suggest that these objects are intrinsically challenging. We also note that two asteroids considered in our analysis are also present in the sample studied by Ďurech & Hanus (2018), namely (205) Martha and (217) Eudora. We do not find an inversion solution for (205), while in the case of (217) our computed period is similar, within 0.007 h (25.2 s), to the Ďurech & Hanus (2018) solution. This is a good agreement for an object that has a period longer than 25 h.

6.2.2. Cellinoid shape model

Table A.3 also lists the results of photometric inversion of GDR2 data using the cellinoid shape model. In this case, the results for the computation of the spin period are slightly better; there are 26 successful inversions out of 39. With respect to the inversions performed using the triaxial shape model, we find the right rotation period also for the asteroids (26), (52), (165), (190), (204), (205), (226), (236), and (350). On the other hand, no good period solution is found for asteroids (79), (188), (217), (277), (388), and (445), which were inverted using the triaxial ellipsoid model. It is not clear why some objects for which no good period solution

is found using the more realistic cellinoid shape model, can be inverted using a simpler triaxial ellipsoid shape model, although as expected the opposite situation occurs more frequently. We also note that in several unsuccessful cases the derived period solution turns out to be about one-half the correct value; we can hardly explain this result at the moment. We also note that in the case of the two asteroids (205) and (217), which were also analyzed by [Durech & Hanus \(2018\)](#), the situation is the opposite of what we find in this work using the triaxial ellipsoid shape model: we find the correct period solution for (205), within less than 0.008 h with respect to the 14.9117 solution of [Durech & Hanus \(2018\)](#). In the case of (217), no good inversion solution is found using the cellinoid shape model.

Despite a better result in terms of number of correct spin period determinations, the pole solutions obtained using the cellinoid shape model tend to be worse; however they do not always disagree with most ground-based determinations. In several cases the pole solution is similar to values found in the literature, but the sense of rotation turns out to be inverted. As in the case of the inversion of HIPPARCOS data, we think that these discrepancies can be due to differences in the inversion algorithm procedure, i.e. the genetic approach is a global optimization method, compared with the locally optimized Levenberg-Marquardt method used to deal with cellinoid shapes. As a possible improvement, we plan to adopt a genetic algorithm to the case of these shapes as well. The effectiveness of such an approach will need extensive testing because of the larger number of parameters to be determined owing to the increased number of different semi-axes describing the cellinoid shape.

7. Conclusions and future work

The main results of the present analysis, and its most immediate consequences can be summarized as follows.

The use of an algorithm including a treatment of a Lommel-Seeliger scattering law computed for triaxial ellipsoid objects makes it possible to obtain only some marginal improvement with respect to the purely geometric scattering approach adopted by [Cellino et al. \(2009\)](#) in the treatment of HIPPARCOS data. This concerns the now successful determination of the rotation period of (18) Melpomene and a few cases in which photometric inversion now gives some pole solutions slightly more compatible with ground-based estimates, with respect to what was found by [Cellino et al. \(2009\)](#).

The attempts of computing photometric inversion using a more realistic shape model, the so-called cellinoids give generally better results for what concerns the determination of the rotation period, whereas in its current version it seems to have problems deriving accurate pole solutions.

A number of tests performed to better analyze the behaviour of the genetic algorithm using triaxial ellipsoid shapes indicates that inversion failures are not simply due to an insufficient number of inversion attempts. Based on experiments in which the number of genetic attempts was allowed to be much higher, we rather conclude that the inversion fails because the corresponding data sets are simply not compatible with the assumed shape model.

It is difficult to conclude that about 50% of relatively large asteroids have shapes so exotic that they cannot be adequately fit by a triaxial ellipsoid shape model. Conversely, a very elongated object as (216) Kleopatra is a good example of a body for which even a very small number of sparse photometric data is sufficient to infer its spin properties correctly, either using old HIPPARCOS data or a small set of new *Gaia* data. It rather seems, therefore,

that at least as far as the asteroids present in the HIPPARCOS catalogue are concerned, the inversion failures mostly concern relatively big and bright objects, which most likely have overall regular shapes. Inversion failures therefore seem to be most probably a consequence of poor data quality.

As a rule, GDR2 data available for those objects observed by HIPPARCOS are not sufficiently abundant to be used alone for photometric inversion purposes. There are, however, two HIPPARCOS targets for which the correct rotation period can be determined from an inversion of a very small number of GDR2 measurements of the order of or smaller than 20, covering limited intervals of ecliptic longitudes. These two objects are (216) Kleopatra and (511) Davida. The successful inversion of Kleopatra is particularly surprising because of the very low number of available GDR2 data.

The failure to successfully invert GDR2 photometric data for some relatively large and bright asteroids using the triaxial shape model seems to be due to the shape model itself. Many of these objects are successfully inverted (at least in terms of determination of the right rotation period) using the cellinoid model. This suggests that in cases in which the number and distribution of available data are not optimal, as in the case of GDR2 data, a more realistic shape model has some advantage over a much simpler, triaxial ellipsoid shape model. On the other hand, we have also found cases of GDR2 asteroids that are successfully inverted using a triaxial shape model, but not using a more complex shape model. The role played by the random sampling of different observing circumstances is important when the number of available observations is small. Some data distributions can be more or less favourable than others for a successful photometry inversion, either using an a priori adopted shape model or using the data to solve for a general convex shape, in addition to the spin parameters. We note there is an intersection of only two asteroids between our sample of 39 analyzed objects (chosen from those numbered up to 500 with more than 25 GDR2 measurements) and the much larger sample of GDR2 asteroids successfully inverted by [Durech & Hanus \(2018\)](#). This means that no satisfactory solution could be found by the latter authors for many of the asteroids for which we found the correct period, using either the triaxial ellipsoid (23 asteroids) or the cellinoid shape model (26 asteroids).

It should also be noted that several GDR2 objects for which no correct inversion solution could be found in the present analysis are fairly bright; as a consequence of their physical sizes and distances, their recorded signals may present at least in some cases non-negligible angular sizes because their light is spread over a larger area of the CCD detectors with respect to the case of point-like sources. This makes them generally not optimal targets for *Gaia* photometric measurements because the pipeline of *Gaia* data reduction is expected to provide its best results for point-like and rather faint (G mag > 12) targets. We should not forget, moreover, that the simple fact that asteroids move during their transits on the *Gaia* focal plane makes them particularly difficult targets for *Gaia* and requires special data reduction procedures. In GDR2 a large number of photometric data were discarded owing to apparently abnormal values of the (unpublished) colour indexes, presumably due to the motion in the *Gaia* focal plane ([Cellino et al. 2018](#)). It is possible that the development of better algorithms for photometric data reduction for solar system objects will improve the quality of *Gaia* photometric data of asteroids in the future data releases. In spite of all the above-mentioned difficulties, we can already obtain a correct photometric inversion for objects for which we have very small numbers of GDR2 photometric data. This suggests that the photometric

accuracy of GDR2 data, which passed several science verification tests to qualify for publication, is very accurate in most cases and is compatible with mission requirements. This is also a major conclusion of the analysis by Āurech & Hanus (2018).

It is possible that some of the bright and large objects for which we could not obtain a correct inversion might have a photometric variation determined by other properties in addition to pure shape effects. Surface albedo variegation, which is not taken into account by the photometric inversion algorithm, can be a possible explanation. A classical example is that of (4) Vesta observed by HIPPARCOS, but more complicated situations than simple albedo variation can also occur in principle.

The cellinoid shape model is the first natural improvement with respect to the adoption of a simpler triaxial ellipsoid. Attempts are currently being made to develop faster inversion algorithms based on the cellinoid shape model, although they still consume too much execution time to be adopted as the photometric inversion algorithm by the *Gaia* DPAC. At the same time, because our results suggest that the estimate of the asteroid poles gives lower quality results than using the simpler triaxial ellipsoid shape, we hope that some more extensive debugging, including more accurate computations of the rotation axis resulting from a given shape, (the axis corresponding to the maximum moment of inertia) will improve the situation.

We absolutely agree with Āurech & Hanus (2018) about the fact that the preliminary analysis of GDR2 photometric data for asteroids allow us to have very high expectations about the role that *Gaia* observations of asteroids published in the next data releases will play in asteroid science.

According to a recent analysis by Bartczak & Dudziński (2019), some essential physical parameters of asteroids, including shape, volume, and density, which are derived by analysis of photometric data, are affected by much larger uncertainties than previously believed. In this respect, the growing data set of extremely high-quality *Gaia* photometric measurements can open a new era in this field. We must be aware that we should not be hasty in profiting from these magnificent data. Their exploitation is a typical end-of-mission task because each single photometric snapshot is extremely important for the purposes of photometric inversion. It is clear that the final *Gaia* data catalogue, which will include preliminary photometric inversions based on a triaxial ellipsoid shape model, will be a very useful starting point. This catalogue will provide a wealth of results to be used for statistical purposes and to attack some specific problems, including for instance the measurement of a Yarkovsky-dominated evolution of the members of asteroid dynamical families. More refined analyses of *Gaia* data will certainly follow, including reliable determination of accurate convex shapes, possibly merging information coming from different sources, such as *Gaia* data, ground-based light curves, and star occultations. At this stage, we think that our approach aimed at avoiding any possible overestimation of the results obtained by analyzing the still small and preliminary GDR2 data set is correct.

As the number of *Gaia* photometric measurements per object will increase in subsequent years of operations, we expect the quality of the results of photometric inversion to increase sensibly as a consequence of improvements in the algorithms of photometric data processing and calibration.

Moreover, we plan to implement methods to derive the values of the (H , G_1 , G_2) parameters of the asteroid photometric

system from available data. These parameters describe how the brightness of the objects changes when they are observed at different phase angles. The H parameter is the absolute magnitude, namely the (normalized to unit distance) magnitude measured at zero phase angle. One of the limitations of *Gaia* is that it cannot observe solar system objects at phase angles smaller than about 10° . The analysis of the available measurements at larger phase angles can, however, lead at least to the determination of the G_1 and G_2 parameters. This could be important because these parameters seem to be related to the geometric albedo of the surface (Belskaya & Shevchenko 2000) and to taxonomic classification (Shevchenko et al. 2016). In case of success, the inversion of *Gaia* photometric data will produce even richer scientific output than the simple determination of spin properties and overall shapes.

Acknowledgements. A.C. thanks the IMCCE and the Paris Observatory for inviting him to work on this project as an Invited Researcher. X.-P.L. is supported under the grant No. 0018/2018/A from the Science and Technology Development Fund, Macau SAR. The authors thank an anonymous referee for his/her comments, which were useful to improve this paper in many respects.

References

- Bartczak, P., & Dudziński, G. 2019, *MNRAS*, **485**, 2431
 Belskaya, I. N., & Shevchenko, V. G. 2000, *Icarus*, **147**, 94
 Carbognani, A., Tanga, P., Cellino, A., et al. 2012, *Planet. Space Sci.*, **73**, 80
 Cellino, A., Zappalà, V., & Farinella, P. 1989, *Icarus*, **78**, 298
 Cellino, A., Delbò, M., Zappalà, V., Dell’Oro, A., & Tanga, P. 2006, *Adv. Space Res.* **38**, 2000
 Cellino, A., Hestroffer, D., Tanga, P., Mottola, S., & Dell’Oro, A. 2009, *A&A*, **506**, 935
 Cellino, A., Muinonen, K., Hestroffer, D., & Carbognani, A. 2015, *Planet. Space Sci.*, **118**, 221
 Cellino, A., Ammannito, E., Magni, G., et al. 2016, *MNRAS*, **456**, 248
 Cellino, A., Berthier, J., Delbò, M., et al. 2018, *Gaia* DR2 documentation, European Space Agency; Gaia Data Processing and Analysis Consortium, 4, Available at <https://gea.esac.esa.int/archive/documentation/GDR2/>
 Āurech, J., & Hanuš, J. 2018, *A&A*, **620**, A91
 Āurech, J., Sidorin, V., & Kaasalainen, M. 2010, *A&A* **513**, A46
 Āurech, J., Carry, B., & Delbo, M. 2015, *Asteroids IV*, eds. P. Michel, F. E. DeMeo, & W. F. Bottke (Tucson, AZ: University of Arizona Press), 183
 Āurech, J., Hanuš, J., Oszkiewicz, D., & Vančo, R. 2016, *A&A*, **687**, A48
 Āurech, J., Hanuš, J., Brož, M., et al., 2018, *Icarus*, **304**, 101
 Gaia Collaboration (Spoto, F., et al.) 2018, *A&A*, **616**, A13
 Hanuš, J., Āurech, J., Oszkiewicz, D. A., et al. 2016, *A&A*, **586**, A108
 Hestroffer, D., Morando, B., Hog, E., et al. 1998, *A&A*, **334**, 325
 Lu, X.-P., Cellino, A., Hestroffer, D., & Ip, W.-H. 2016, *Icarus*, **267**, 24
 Migliorini, F., Manara, A., Scaltriti, F., et al. 1997, *Icarus*, **128**, 104
 Muinonen, K., Wilkman, O., Cellino, A., et al. 2015, *Planet. Space Sci.*, **118**, 227
 Pravec, P., & Harris, A.W. 2000, *Icarus*, **148**, 12
 Pravec, P., & Harris, A.W. 2018, Asteroid Lightcurve Data Base (LCDB) V2.0 urn:nasa:pds:ast-lightcurve-database::2.0, NASA Planetary Data System
 Pravec, P., Harris, A.W., & Michalowski, T. 2002, *Asteroids III*, eds. W. F. Bottke, A. Cellino, P. Paolicchi, & R. P. Binzel (Tucson, AZ: University of Arizona Press), 113
 Santana-Ros, T., Bartczak, P., Michalowski, T., Tanga, P., & Cellino, A. 2015, *MNRAS*, **450**, 333
 Shevchenko, V. J., Belskaya, I. N., Muinonen, K., et al. 2016, *Planet. Space Sci.*, **123**, 101
 Torppa, J., Valkkonen, J. P. T., & Muinonen, K. 2006, *Potato Res.*, **49**, 109
 Torppa, J., Hentunen, V.-P., Pääkkönen, P., Kehusmaa, P., & Muinonen, K. 2008, *Icarus*, **198**, 91
 van Leeuwen, F., de Bruijne, J. H. J., Arenou, F., et al. 2018, Gaia DR2 documentation, European Space Agency; Gaia Data Processing and Analysis Consortium, Available at <https://gea.esac.esa.int/archive/documentation/GDR2/>

Appendix A: Tables

Table A.1. Results of photometric inversion of HIPPARCOS data for asteroids, using the triaxial ellipsoid shape model.

Object number	No. of HIPPARCOS measurements (total)	Known rotation period (h)	Rotation period from inversion (h)	Pole coordinates from inversion (λ, β)	b/a	c/a	No. of used measurements	Max accepted error for HIPPARCOS data (mag)
1	65	9.074170	–	–	>0.97	>0.79	65	0.03
2	62	7.8132	–	(202,+55)	0.88	0.84	56	0.03
3	60	7.210	(7.2867)	(93,+52)	0.87	0.50	58	0.03
4	58	5.34212767	10.6826	(340,+70)	0.91	0.55	58	0.03
5	70	16.801	16.8015	(323,+64)	0.80	0.80	43	0.03
6	91	7.2745	(14.7910)	(345,+50)	0.90	0.78	85	0.03
7	69	7.139	–	–	–	–	66	0.03
8	55	12.865	–	–	–	–	41	0.03
9	40	5.079	–	–	–	–	47	0.04
10	48	27.630	27.6621 ⁽¹⁾	(196,–48)	0.68	0.66	47	0.04
			27.6611	(315,–90)	0.78	0.15		
11	64	13.7204	–	–	–	–	46	0.03
13	29	7.045	–	–	–	–	29	0.05
14	42	15.028	–	–	–	–	31	0.03
15	82	6.083	6.0828	(309,–53)	0.70	0.67	63	0.03
			6.0828	(109,–64)	0.71	0.71		
16	41	4.196	–	–	–	–	41	0.05
18	93	11.570	11.5706 ⁽²⁾	(24,+19)	0.83	0.83	55	0.03
			11.5705	(195,+36)	0.83	0.83		
20	57	8.098	8.0975	(36,+41)	0.82	0.82	48	0.04
			8.0996	(47,–34)	0.83	0.83	39	0.03
			10.2840	(30,+85)	0.83	0.15		
22	50	4.1483	(4.273)	(02,+14)	0.70	0.62	26	0.03
23	46	12.312	–	–	–	–	46	0.05
27	32	10.4082	–	–	–	–	32	0.05
29	73	5.3921	–	–	–	–	64	0.03
			–	–	–	–	71	0.04
30	35	13.686	– ⁽³⁾	–	–	–	35	0.05
39	109	5.138	5.1383 ⁽⁴⁾	(333,+52)	0.70	0.39	83	0.03
40	73	8.910	8.9108	(202,–18)	0.73	0.73	38	0.03
42	49	13.590	13.5832	(110,+42)	0.76	0.54	41	0.03
44	49	6.422	6.4215	(296,+49)	0.66	0.50	29	0.03
88	31	6.042	–	–	–	–	31	0.05
129	37	4.9572	–	–	–	–	37	0.05
192	28	13.625	(13.3807)	(100,–78)	0.87	0.16	28	0.05
			13.6252	(99,–78)	0.86	0.16		
216	19	5.385	5.3852	(238,+26)	0.43	0.35	19	0.05
			5.3851	(59,–11)	0.43	0.34		
230	32	24.0055	–	–	–	–	32	0.05
324	67	29.43	–	–	–	–	67	0.05
349	88	4.701	4.6933	(356,–64)	0.80	0.68	64	0.03
			4.7012 ⁽⁵⁾	(152,+44)	0.78	0.72	63	0.03
			4.7012	(324,+28)	0.77	0.72		
354	86	4.277	(4.44)	(145,+49)	0.74	0.56	50	0.03
471	94	7.113	7.1278	(222,+54)	0.86	0.53	80	0.04
			7.1152	(226,+59)	0.85	0.47		
			7.1152	(227,+58)	0.84	0.48	51	0.03
511	47	5.1297	–	–	–	–	46	0.05
532	39	9.405	–	–	–	–	39	0.05
704	77	8.727	– ⁽⁶⁾	–	–	–	35	0.03

Notes. With the exception of (216) Kleopatra, we only consider asteroids having a number of HIPPARCOS measurements >25. Some P solutions that are different from, but close to, the correct solution are given in brackets. Some pole solutions are listed, when close to ground-based estimates, also for a few objects for which the derived spin period solution is wrong, and/or very close to twice the ground-based derived period. No error bars are indicated for the obtained period and pole coordinates solutions, for the reasons explained in the text. Note that the inversion results do not change if the value for the maximum accepted photometric error for the HIPPARCOS measurements, given in the last column, are changed. ⁽¹⁾Same P using 0.03 mag error limit. Best P solution always in competition with alternative solution having $P = 37.5$ h. ⁽²⁾After removal of three brightest HIPPARCOS data at ecliptic longitude $\lambda \approx 280^\circ$. ⁽³⁾The correct solution with $P = 13.68$ is found, but it is not the best solution. ⁽⁴⁾Alternative solutions exist and give similar (although nominally worse) residuals. ⁽⁵⁾After removal of brightest HIPPARCOS mag. ⁽⁶⁾A solution with $P = 8.70$ h appears, but it gives worse residuals than several bad solutions.

Table A.2. Same as Table A.1, but the listed results are those obtained using a more complex, cellinoid shape model.

Object number	No. of HIPPARCOS measurements (total)	Known rotation period (h)	Rotation period from inversion (h)	Pole coordinates (λ, β)	No. of used measurements	Max accepted error for HIPPARCOS data (mag)
1	65	9.074170	(18.1274) ⁽¹⁾	–	65	0.03
2	62	7.8132	–	–	56	0.03
3	60	7.210	–	–	58	0.03
4	58	5.34212767	10.6827	(157,–67)	58	0.03
5	70	16.801	–	–	43	0.03
6	91	7.2745	7.2761	348,+46	85	0.03
7	69	7.139	–	–	66	0.03
8	55	12.865	–	–	41	0.03
9	40	5.079	–	–	47	0.04
10	48	27.630	27.6581	(45,+50)	47	0.04
11	64	13.7204	–	(140,+23)	46	0.03
13	29	7.045	–	–	29	0.05
14	42	15.028	–	–	31	0.03
15	82	6.083	6.0827	(160,+69)	63	0.03
16	41	4.196	–	–	41	0.05
18	93	11.570	–	–	55	0.03
20	57	8.098	8.0973	(61,+43)	48	0.04
22	50	4.1483	–	–	26	0.03
23	46	12.312	–	–	46	0.05
27	32	10.4082	–	–	32	0.05
29	73	5.3921	5.3893	(151,+60)	64	0.03
30	35	13.686	13.6854	(252,+31)	35	0.05
39	109	5.138	(4.9543)	(311,–23)	83	0.03
40	73	8.910	8.9132	(19,+82)	38	0.03
42	49	13.590	13.5905	(288,–01)	41	0.03
44	49	6.422	6.4215	(108,–30)	29	0.03
88	31	6.042	–	–	31	0.05
129	37	4.9572	4.9570	(264,–05)	37	0.05
192	28	13.625	–	–	28	0.05
216	19	5.385	5.3862	(255,+57)	19	0.05
230	32	24.0055	–	–	32	0.05
324	67	29.43	–	–	67	0.05
349	88	4.701	4.7012	(328,–44)	64	0.03
354	86	4.277	–	–	50	0.03
471	94	7.113	7.1152	(29,+01)	80	0.04
511	47	5.1297	5.1296	(307,+33)	46	0.05
532	39	9.405	–	–	39	0.05
704	77	8.727	–	–	35	0.03

Notes. This shape model has more complicated axial ratios that are not listed. ⁽¹⁾Obtained P is very close to twice the correct value.

Table A.3. Results of photometric inversion of GDR2 photometric data for asteroids numbered up to 500, using both a regular triaxial ellipsoid shape model and a cellinoid shape model.

Object	No. of GDR2 measurements	Known Rotation period (h)	Rotation period (h) from data inversion (triaxial ellipsoid)	Rotation period (h) from data inversion (cellinoid shape)	Notes
216	17	5.385	5.3854	5.3855	Present also in HIPPARCOS data set. Triaxial ellipsoid pole consistent with ground-based determinations.
511	23	5.1297	5.1300	5.1290	Present also in HIPPARCOS data set. Possible inversion of sense of spin in the triaxial ellipsoid solution.
26	39	13.110	–	13.1106	Pole solution compatible with ground-based estimates, but with inverted sense of rotation.
48	32	11.89	11.8946	11.8903	Cellinoid pole solution compatible with ground-based estimates, but with inverted sense of rotation.
52	28	5.6304	–	5.6248	Pole solution different from ground-based determinations.
54	28	7.024	7.0117	7.0224	Pole ambiguity.
79	36	5.978	5.9601	–	Pole longitude 180° ambiguity.
95	30	8.705	8.7015	8.7049	Pole ambiguity.
123	26	10.04	–	–	Multiple solutions, no good one.
154	41	25.224	25.2672	25.2481	Triaxial ellipsoid shape finds an opposite sense of spin with respect to (few) ground-based estimates.
155	28	7.9597	7.9592	7.9592	Poor agreement with ground-based pole solutions.
156	33	22.37	–	–	Best solutions give $P = 22.11$ h.
159	36	24.476	24.4792	24.4780	Pole unknown for this object.
165	31	7.226	–	7.1723	Pole solution in agreement with ground-based estimates.
183	31	11.77	11.7691	11.7690	Triaxial ellipsoid pole solution in partial agreement with ground-based estimates.
188	26	11.98	11.9770	–	Pole solution in partial agreement with ground-based estimates.
190	28	6.52	–	6.5187	Pole solution not very far from ground-based estimates, but inverse sense of rotation.
204	38	19.489	–	19.4868	Pole unknown for this object.
205	46	14.911	–	14.9039	Pole unknown for this object.
213	41	8.045	–	–	Pole unknown for this object.
217	29	25.272	25.2553	–	An alternative period solution exists. Pole unknown.
226	36	11.147	–	11.1436	Pole longitude 180° away from published ground-based solution.
236	33	12.336	–	12.3452	Computed pole far from (only one) ground-based solution.
260	28	8.29	8.2904	8.2905	Good agreement with ground-based pole solution.
264	31	9.2276	–	–	Strange ecliptic longitude – mag data distribution.
271	31	18.787	18.7866	18.7866	Good agreement with ground-based pole solution.
276	34	6.315	6.3191	6.3195	Good agreement with ground-based pole solution.

Notes. Only asteroids that have a number of *Gaia* measurements >25 are listed. The exceptions are (216) Kleopatra and (511) Davida, for which HIPPARCOS data were also available. As shown in Table A.1, HIPPARCOS-based inversion was successful for Kleopatra and unsuccessful for Davida, whereas using GDR2 data, this asteroid can be successfully inverted as well. No estimate of the error bars in the obtained periods are given for the reasons explained in the text.

Table A.3. continued.

Object	No. of GDR2 measurements	Known Rotation period (h)	Rotation period (h) from data inversion (triaxial ellipsoid)	Rotation period (h) from data inversion (cellinoid shape)	Notes
277	30	29.69	29.6927	–	Pole in agreement with some ground-based solutions.
295	32	10.730	21.4103	10.7055	Triaxial ellipsoid solution gives $P \approx 2P(\text{ground-based})$. Pole unknown for this object.
300	28	6.8423	–	–	Pole unknown for this object.
318	29	42.49	–	–	Pole unknown for this object.
323	26	9.463	–	–	Pole unknown for this object.
340	51	8.0062	8.0060	8.0062	Cellinoid pole close ground-based solution. Uncertain sense of spin.
348	31	7.3812	7.3835	7.3840	More than one pole solution. Pole unknown for this object.
350	38	9.178	–	9.1817	Pole solution in agreement with ground-based estimate.
362	28	16.92	16.9272	16.9256	Alternative P solutions exist for triaxial ellipsoid shape. Cellinoid pole solution far from ground-based estimate.
388	27	9.516	9.5124	–	Equivalent (slightly better) period solutions exist. Pole unknown for this object.
399	37	9.136	9.1463	9.1463	Different pole solutions.
411	30	11.344	22.7024	10.4431	Triaxial ellipsoid solution gives $P \approx 2P(\text{ground-based})$. Different pole solutions, all in disagreement with ground-based estimates.
441	36	10.446	10.4430	10.4431	Triaxial ellipsoid pole solution in good agreement with ground-based solutions.
445	29	19.97	19.9762	–	Pole unknown for this object.